JACS Au
AN OPEN ACCESS JOURNAL OF THE AMERICAN CHEMICAL SOCIETY

pubs.acs.org/jacsau

Article

Transforming Chemical Proteomics Enrichment into a High-Throughput Method Using an SP2E Workflow

Tobias Becker, Andreas Wiest, András Telek, Daniel Bejko, Anja Hoffmann-Röder, and Pavel Kielkowski*

Cite This: *JACS Au* 2022, 2, 1712–1723

Read Online

ACCESS | Metrics & More | Article Recommendations | Supporting Information

ABSTRACT: Protein post-translational modifications (PTMs) play a critical role in the regulation of protein catalytic activity, localization, and protein–protein interactions. Attachment of PTMs onto proteins significantly diversifies their structure and function, resulting in proteoforms. However, the sole identification of post-translationally modified proteins, which are often cell type and disease-specific, is still a highly challenging task. Substoichiometric amounts and modifications of low abundant proteins necessitate the purification or enrichment of the modified proteins. Although the introduction of mass spectrometry-based chemical proteomic strategies has enabled the screening of protein PTMs with increased throughput, sample preparation remains highly time-consuming and tedious. Here, we report an optimized workflow for the enrichment of PTM proteins in a 96-well plate format, which could be extended to robotic automation. This platform allows us to significantly lower the input of total protein, which opens up the opportunity to screen specialized and difficult-to-culture cell lines in a high-throughput manner. The presented SP2E protocol is robust and time- and cost-effective, as well as suitable for large-scale screening of proteoforms. The application of the SP2E protocol will thus enable the characterization of proteoforms in various processes such as neurodevelopment, neurodegeneration, and cancer. This may contribute to an overall acceleration of the recently launched Human Proteoform Project.

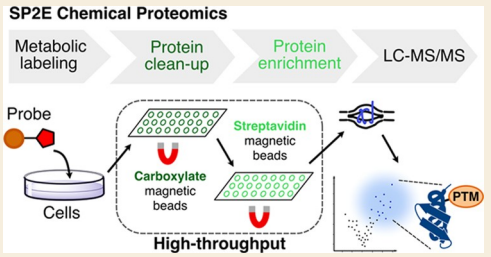

KEYWORDS: *chemical proteomics, SP3, protein post-translational modifications, AMPylation, glycosylation*

INTRODUCTION

Protein post-translational modifications (PTMs) are crucial for the regulation and fine-tuning of many important biological processes such as neurodevelopment,[1−4] circadian clocks,[5] aging,[6] and impairment in numerous diseases.[7−9] The incredible diversity of genetic polymorphism, RNA splice variants, and PTMs results in many proteoforms,[4,10,11] which exceed the ∼20,000 human genes by approximately 50 times. This biological network orchestrates the most complex processes including brain development and ensures a dynamic response of the cells to an external stimulus. However, the extent of protein PTMs in laboratory-cultured cells can differ significantly depending on cell types, diseases, and culture conditions. Mass spectrometry (MS)-based chemical proteomics has allowed to reliably map protein PTMs across various experimental conditions.[12−17] A widespread application of the chemical proteomic strategy was enabled by parallel improvements of liquid chromatography technologies, gains in speed, and sensitivity of mass spectrometers and bioinformatic pipelines for protein identification and quantification.[18−21] Nowadays, chemical proteomics is used to uncover the scope of protein PTMs in different cell types by the development of small-molecule probes, which mimic their natural counterparts. The utilization of these probes has provided valuable insights into protein acetylation, palmitoylation, myristoylation, prenylation, glycosylation, ADP-ribosylation, and AMPylation.[1,12−14,22−25] In general, different chemical proteomic workflows follow the same sequence of key steps (Figure 1A). First, cultured cells are treated with the probe, which infiltrates the cellular system and competes with the endogenous substrate for the active site of the PTM writer enzymes. Next, the chemical proteomic probes contain an alkyne or azide handle to facilitate a bioorthogonal coupling to suitable biotin linkers with either Cu-catalyzed alkyne–azide cycloaddition (CuAAC) or copper-free strain-promoted azide–alkyne cycloaddition (SPAAC), respectively.[15,26] Following the click chemistry, proteins are precipitated to remove the excess biotin reagents and nonprotein components of the cell lysate.[1,13] In the next step, biotin-labeled proteins are enriched using avidin-coated beads. The critical part of this step is to maximize the efficiency of the washing to remove nonspecifically bound proteins and thus to reduce the complexity of the final MS sample while improving ratios

Received: May 9, 2022
Revised: June 3, 2022
Accepted: June 3, 2022
Published: June 30, 2022

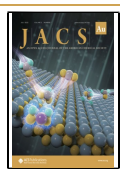

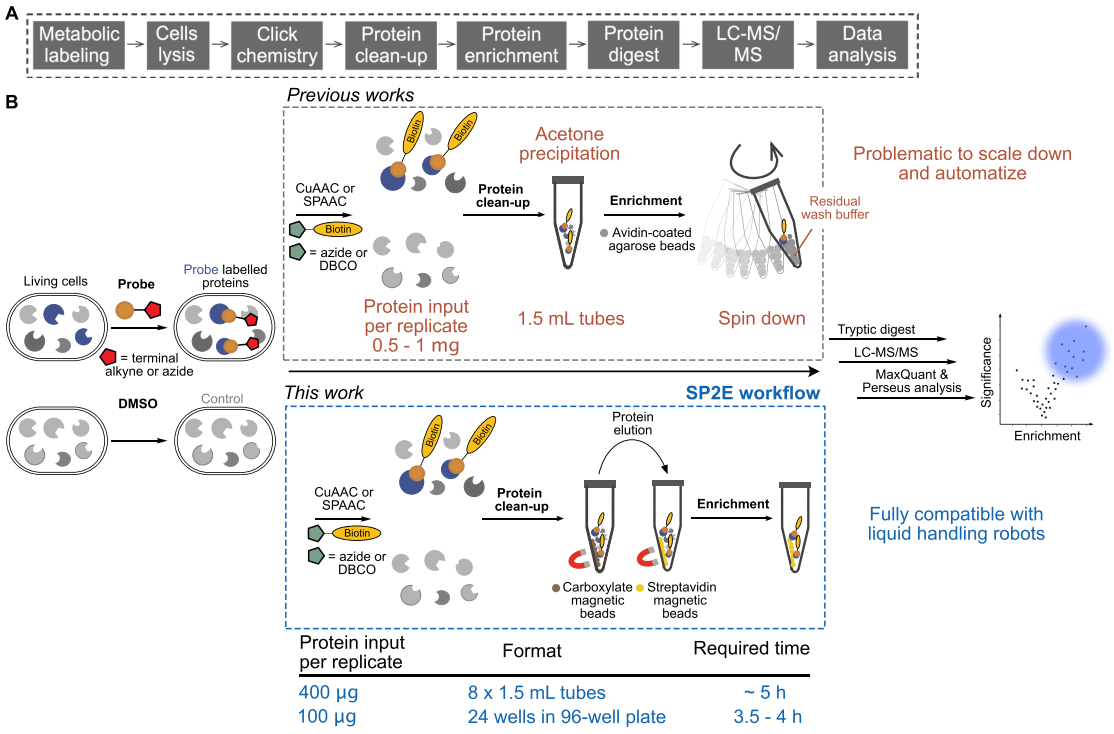

Figure 1. Schematic overview of the chemical proteomic workflow. (A) Key steps of the standard chemical proteomic workflow and (B) schematic characterization of the SP2E workflow and basic parameters of the procedure in comparison to the previously used workflow with avidin-coated agarose beads. In the table below the SP2E workflow, the typical times required to proceed with 8 samples (large scale) or 24 samples (small scale) are shown. For comparison, the previously used workflow would typically take about 8 h for eight samples.

between control- and probe-treated samples. After reduction and alkylation of the enriched modified proteins, they are digested by trypsin or another protease, desalted and concentrated for MS measurement.[27] Subsequently, each sample is measured separately for the label-free quantification (LFQ), providing the possibility to add more samples into the data set later on.[28] MS data are typically acquired on orbitrap or timsTOF-based liquid chromatography-tandem mass spectrometry (LC-MS/MS) instruments. Finally, peptide and protein identifications and quantifications are carried out using well-established commercial or free-of-charge pipelines such as MaxQuant or MSFragger.[21,28] A comparison of the probe-treated and control cells allows us to distinguish between unspecific protein binders and probe-modified proteins. Despite the success of chemical proteomic technology, the community of scientists combining organic synthesis, mass spectrometry, and biology is still rather small. With numerous validated commercial PTM probes and the widespread availability of mass spectrometers either used in individual groups or as a core service, the bottlenecks of the chemical proteomic approach still remain in the insufficient consistency, time inefficiency, and laboriousness of the enrichment techniques. Furthermore, the emerging field of chemical proteomic studies focused on neurodevelopment and the complex environment of the central nervous system composed of many different cell types is not compatible with the high amounts of total proteins that are required for the analysis so far. In a perfect scenario, the workflow would be efficient and reproducible even with a low protein input and the enrichment would require a minimum hands-on time or full automation. In comparison to standard MS whole proteome sample preparation methods, which include filter-assisted sample preparation (FASP), in-StageTip digestion (iST), and single-pot solid-phase-enhanced sample preparation (SP3), the chemical proteomic method not only requires highly efficient protein and peptide purification but also needs to be combined with suitable bioorthogonal reaction conditions and much higher starting protein amounts (Figure 1B).[29−32] Thus far, the most common chemical proteomic methods for protein PTM enrichment utilize acetone or chloroform−methanol precipitation to remove the excess of click chemistry reagents.[13] Further, enrichment with avidin-coated agarose beads requires centrifugation or filtration to separate them from the wash buffer, which hinders the scale down and robotic automation of the approach. Of note, the Tate group combined avidin-coated magnetic beads and a trifunctional linker with azide, biotin, and rhodamine to visualize the enriched proteins by in-gel analysis,[13,33] and recently, the Backus group has implemented the SP3 peptide clean up into their chemical proteomic workflow before transferring the peptides including the biotin-modified peptides on avidin-coated agarose beads.[34] Although similar affinity enrichment techniques combined with MS have been reported, to our best knowledge, a procedure feasibly integrating all aspects of small-scale chemical proteomics is not available.[35,36]

Here, we report the development and optimization of a chemical proteomic method, which uses carboxylate-modified magnetic beads to clean up the proteins after CuAAC and streptavidin-coated magnetic beads for the enrichment of the labeled proteins (Figure 1B). The new method termed SP2E was further scaled down to a 96-well plate format, starting with 100 μg total protein. The SP2E method has been successfully used for profiling protein glycosylation and the low abundant protein PTM called AMPylation. Together, the SP2E method provides a time-effective and robust platform for the routine and high-throughput profiling of protein PTMs, representing

https://doi.org/10.1021/jacsau.2c00284
JACS Au 2022, 2, 1712−1723

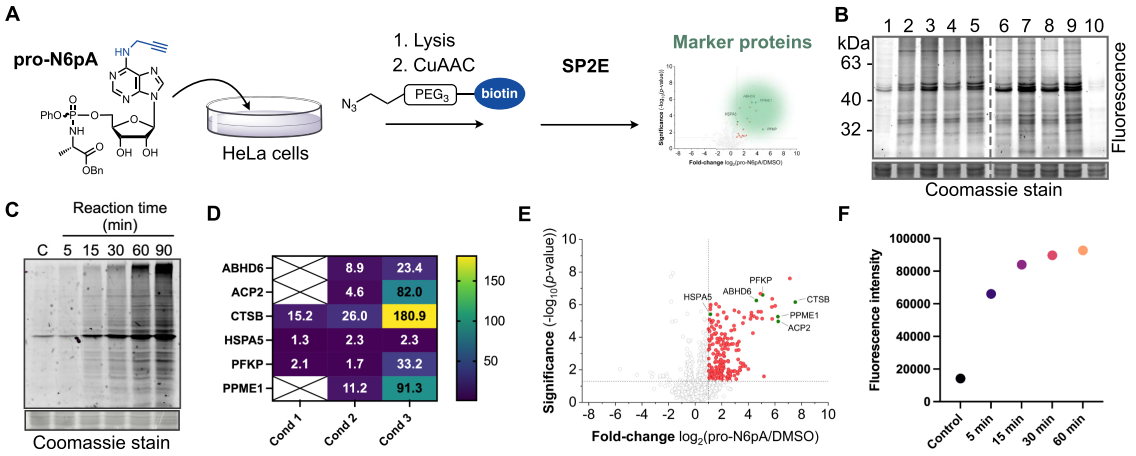

Figure 2. Development and optimization of the SP2E workflow using the AMPylation probe. (A) Pro-N6pA probe structure and the workflow used for the optimization of the SP2E method. (B) Optimization of the lysis buffer based on the efficiency of the CuAAC click chemistry. Lysis buffer compositions: line 1 (control cells treated with plain dimethyl sulfoxide (DMSO) and lysed in 1% NP-40, 0.2% SDS in 20 mM HEPES), line 2 (1% NP-40 in PBS), line 3 (1% NP-40, 0.2% SDS in PBS), line 4 (0.5% Triton in PBS), line 5 (0.5% Triton, 0.2% SDS in PBS), line 6 (1% NP-40 in 20 mM HEPES), line 7 (1% NP-40, 0.2% SDS in 20 mM HEPES), line 8 (0.5% Triton in 20 mM Hepes), line 9 (0.5% Triton, 0.2% SDS in 20 mM Hepes), and line 10 (8 M urea in 0.1 M Tris/HCl). (C) In-gel fluorescence showing the click reaction time optimization. In the control C, cells were treated with plain DMSO and the lysate was incubated with the click reaction mixture for 90 min. (D) Heatmap visualizing the SP2E workflow optimization based on fold enrichment of six marker proteins. Condition 1 (without added urea to the click reaction mixture before protein loading onto carboxylate magnetic beads), condition 2 (with added urea to the click reaction before protein loading onto carboxylate beads and one pot clean up and enrichment of modified proteins), and condition 3 (with added urea into the click reaction, but the spatial separation of the protein clean up and enrichment). The numbers in boxes represent fold enrichments. (E) Volcano plot showing significantly enriched proteins (red dots) using the pro-N6pA AMPylation probe with highlighted marker proteins (green dots) using the optimized SP2E workflow (condition 3 from Figure 2D); $n = 4$, cutoff lines at p-value >0.05 and 2-fold enrichment. (F) Plot displaying total fluorescence intensity from the in-gel analysis of the time optimization of biotin−streptavidin complex formation.

an important step toward the robotic automation of the approach.

RESULTS

Development of the SP2E Workflow for Chemical Proteomics

To implement both carboxylate- and streptavidin-coated magnetic beads for protein clean up after click chemistry instead of precipitation and replacement of avidin agarose beads, every step of the chemical proteomic workflow was optimized. Here, we describe the most critical steps leading to an efficient enrichment of PTM proteins, which include the click chemistry conditions, protein loading on carboxylate magnetic beads, and spatial separation of protein clean up and enrichment. First, we set out to optimize the lysis buffer composition to maximize the efficiency of the click chemistry. To evaluate this, HeLa cells were treated with the cell-permeable pro-N6pA probe infiltrating protein AMPylation (Figure 2A).[1,17] After overnight incubation, the cells were harvested and lysed in nine different lysis buffers (Figure 2B). The CuAAC click chemistry was performed with 200 μg of total protein per sample in 100 μL of the respective lysis buffer and azide−TAMRA to visualize the conversion efficiency by in-gel fluorescence scanning after sodium dodecyl sulfate-polyacrylamide gel (SDS-PAGE) electrophoresis. The overall brightest fluorescence and highest amount of fluorescent protein bands was observed in the lysis buffer containing 1% NP-40, 0.2% SDS in 20 mM *N*-(2-hydroxyethyl)piperazine-*N*′-ethane sulfonic acid (HEPES) pH 7.5 (Figures 2B and S1), which was further used for all following experiments. To complete the click chemistry optimization, a time-dependent experiment was carried out to show that 1.5 h is necessary to maximize the yield of the reaction (Figure 2C). For the following optimization steps of the MS workflow, we used a group of six known AMPylated maker proteins (HSPA5, CTSB, PFKP, PPME1, ACP2, ABHD6) to assess the PTM protein enrichment efficiency. The first optimization step was to examine the influence of the buffer composition on the efficiency of the protein binding to the carboxylate magnetic beads. Therefore, 400 μg of total protein in 200 μL of lysis buffer was used for the click reaction with azide−PEG_3−biotin. After the CuAAC incubation time, the resulting click reaction mixture was directly transferred onto carboxylate-coated magnetic beads and followed by the addition of absolute EtOH to a final concentration of 60% to induce the protein complexation. After washing the beads three times with 80% EtOH, the streptavidin-coated magnetic beads were added directly to the carboxylate-coated magnetic beads and incubated for 1 h in 0.2% SDS in phosphate-buffered saline (PBS) to form the biotin−streptavidin complex. To remove the unmodified proteins, the bead mixture was washed thrice with 0.1% NP-40 in PBS, twice with 6 M urea, and thrice with water. The enriched proteins were subsequently reduced, alkylated, and trypsin digested in ammonium bicarbonate (ABC) buffer. The resulting peptides were eluted from the beads by two washes with ABC buffer before desalting on off-line Sep-Pak C18 columns and separation on a UHPLC using a 150 min gradient with the high-fidelity asymmetric waveform ion mobility spectrometry (FAIMS) device attached on to the Orbitrap Eclipse Tribrid mass spectrometer. The MS data were analyzed by MaxQuant and evaluated in Perseus.[20,28]

We have observed that protein loading onto carboxylate magnetic beads directly in lysis buffer with the click reagents did not give satisfactory results with poor enrichment of the marker proteins (Figures 2D and S2 and Table S1). Therefore,

https://doi.org/10.1021/jacsau.2c00284
JACS Au 2022, 2, 1712−1723

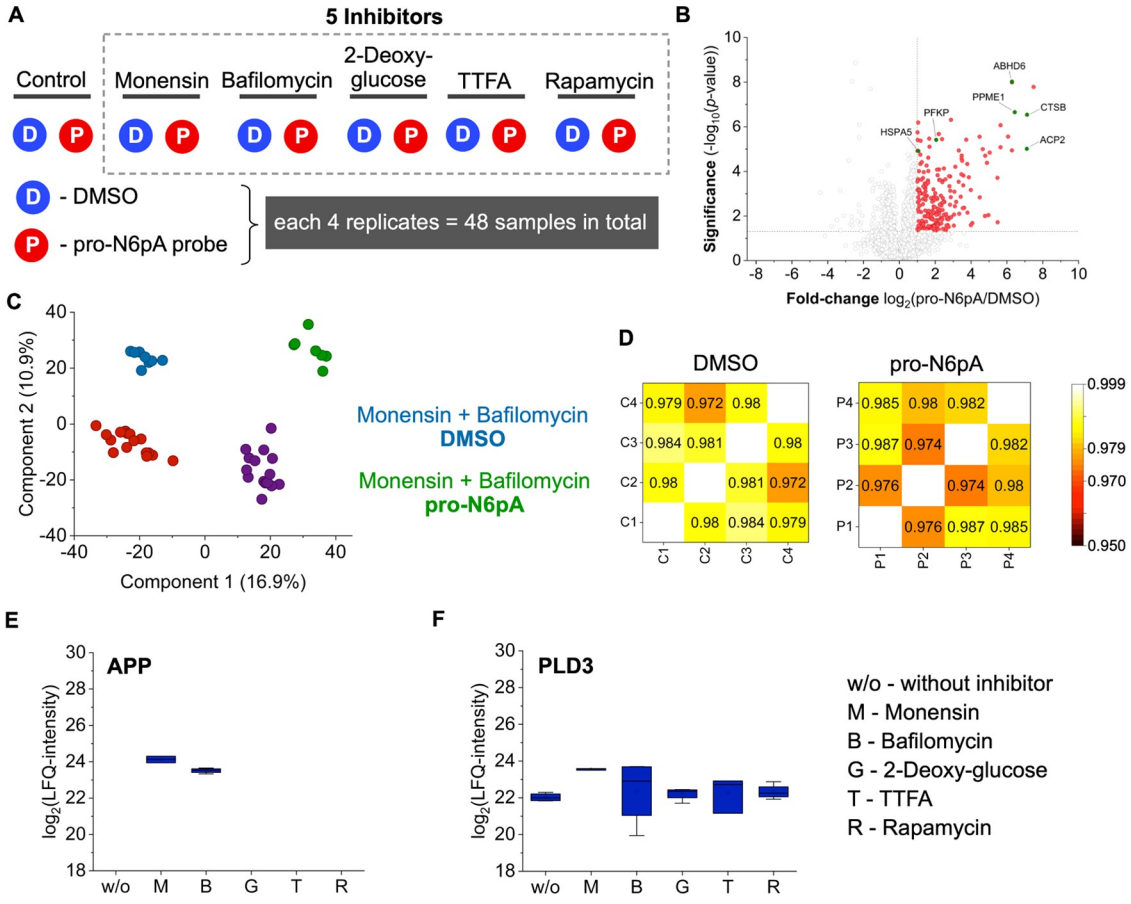

Figure 3. Analysis of protein AMPylation under different stress conditions using the SP2E workflow. (A) Design of the experiment to test the impact of various inhibitors on protein AMPylation. (B) Volcano plot showing the enrichment of AMPylated proteins (pro-N6pA vs DMSO) from SH-SY5Y cells using the SP2E protocol; n = 4, cutoff lines at p-value >0.05 and 2-fold enrichment. (C) PCA of the inhibitor-treated cells and controls displaying separation of the monensin and bafilomycin as well as pro-N6pA-treated cells. Samples that were treated with DMSO and either rapamycin, 2-deoxy-D-glucose, TTFA, or without any inhibitor are depicted in red. Samples that were treated with pro-N6pA and either rapamycin, 2-deoxy-D-glucose, TTFA, or without any inhibitor are depicted in purple. (D) Representative heatmaps visualizing the Pearson correlation coefficients of LFQ intensities of DMSO and pro-N6pA replicates. (E) Profile plot displays the APP LFQ intensities under various conditions. The APP was not found in any other conditions, for example, in cells only treated with DMSO or some other inhibitors. (F) Profile plot displays the PLD3 LFQ intensities under various conditions.

based on our previous experiments, we have tested whether the addition of concentrated urea to the click reaction mixture in advance may improve the protein loading onto the carboxylate magnetic beads. This could be explained by the interference of copper with the protein complexation to carboxylate magnetic beads. Thus, the addition of urea may lead to the neutralization of this effect.[37,38] Indeed, the dilution of the lysis buffer to a final concentration of 4 M urea has significantly improved the overall enrichment ratio (Figures 2D and S3 and Table S2).

Finally, we explored whether it is possible to reduce the overall protein background binding by spatial separation of the protein clean up and enrichment by eluting the proteins from the carboxylate magnetic beads before adding them to the streptavidin-coated magnetic beads in a new tube and thus improve the enrichment ratio. Hence, after the protein clean up on carboxylate magnetic beads, the proteins were eluted twice with 0.2% SDS in PBS and transferred onto streptavidin magnetic beads. The resulting volcano plot confirmed that spatial separation of protein clean up and enrichment is beneficial for PTM protein enrichment and hence outcompetes the advantage of performing both steps in one pot (Figure 2D,E and Table S3). In particular, the enrichment of ACP2 and PFKP has increased by more than 17-fold during the method development. Overall, when compared to the previous benchmark enrichment based on the avidin agarose beads, the optimized SP2E workflow yielded 10-fold more significantly enriched proteins.[17]

Additionally, the protein digest on beads and subsequent peptide elution conditions have been optimized.[31,39] However, standard reduction and alkylation with tris(2-carboxyethyl)-phosphine (TCEP) and chloroacetamide (CAA) at 95 °C for 5 min after the protein enrichment gave satisfying results (Figure 2E). To further shorten the time of the workflow, we analyzed the time dependency of the biotin−streptavidin complex formation to find out that 15 min is sufficient (Figures 2F and S4).

Taken together, we have established the feasible SP2E workflow for the MS-based analysis of PTM proteins. First, we showed that the lysis buffer containing 1% NP-40 and 0.2% SDS in 20 mM HEPES pH 7.5 efficiently lyse the cells and improves the yield of the CuAAC. Furthermore, the addition of urea into the lysis buffer after click chemistry enhances protein loading on the carboxylate magnetic beads. Next, we demonstrated that it is possible to reduce the background by

https://doi.org/10.1021/jacsau.2c00284
JACS Au 2022, 2, 1712−1723

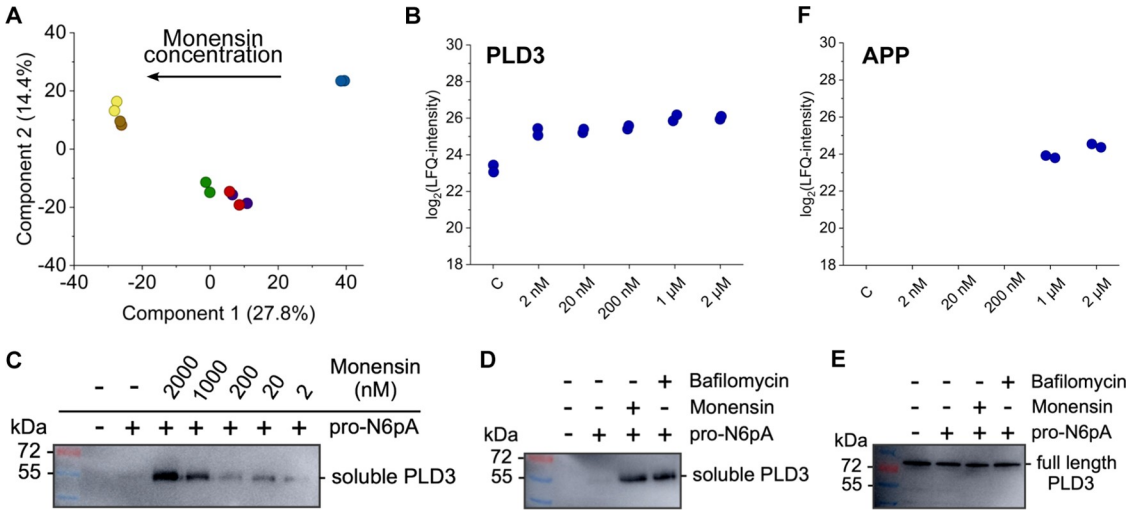

Figure 4. Monensin concentration-dependent increase in APP and PLD3 modification. (A) PCA displays distinct changes in the enriched proteins with increasing monensin concentration. (B) Profile plot of the PLD3 LFQ intensities shows a rapid increase in the PLD3 modification with a 2 nM monensin concentration. (C) Monensin concentration-dependent enrichment of the modified PLD3. For the enrichment, the SP2E protocol was used but the proteins were released from the streptavidin beads by the loading buffer, separated by SDS-PAGE, and analyzed via western blotting with the anti-PLD3 antibody. (D) Enrichment of the modified PLD3 after the treatment with bafilomycin (100 nM) and monensin (2 μM). For the enrichment, the SP2E protocol was used but the proteins were released from the streptavidin beads by loading buffer, separated by SDS-PAGE, and analyzed via western blotting with the anti-PLD3 antibody. (E) Western blotting of the whole proteome from cells treated with bafilomycin (100 nM) and monensin (2 μM) stained with the anti-PLD3 antibody. (F) In contrast to PLD3, the profile plot of the APP LFQ intensity reveals that APP is only enriched with the pro-N6pA probe with 1 and 2 μM monensin in cell culture media.

spatial separation of the protein clean up and enrichment by eluting the proteins from the carboxylate magnetic beads before adding them to the streptavidin magnetic beads. The SP2E workflow utility was demonstrated on productive enrichment of the low abundant AMPylated proteins.

Application of the SP2E Workflow for Analysis of Protein AMPylation

To validate our approach using a heterogeneous set of samples, we went on to investigate metabolic pathways which putatively regulate protein AMPylation. In our previous studies, we showed that primary lysosomal proteins in neuroblastoma SH-SY5Y cells are metabolically labeled by our probe and thus likely AMPylated. Moreover, the profiling of protein AMPylation during neuronal differentiation of the human-induced pluripotent stem cells (hiPSCs) revealed an accumulation of the lysosomal AMPylated proteins in mature neurons, including PLD3, ACP2, and ABHD6.[1,17] In the case of PLD3, the increased AMPylation correlates with a decrease in its exonuclease catalytic activity. However, in parallel, another group of proteins localized to cytosol and mitochondria has been consistently enriched, including PFKP, PPME1, SLC25A3, and cytoskeletal proteins. There are two known AMPylators thus far, FICD and SELENOO, which are localized in the endoplasmic reticulum (ER) and mitochondria, respectively. This raises the question about the localization and mechanism of metabolic or signaling pathways regulated by protein AMPylation apart from the previously described FICD-HSPA5 axis involved in the unfolded protein response (UPR).[6,40,41] With our optimized SP2E workflow, we decided to address this question using a set of five inhibitors blocking mTOR, autophagy lysosomal pathway, glycolysis, and cellular respiration. Therefore, the neuroblastoma SH-SY5Y cells were treated with rapamycin, bafilomycin, 2-deoxy-D-glucose, thenoyltrifluoroacetone (TTFA), and monensin.[42−46] SH-SY5Y cells were treated either with the inhibitor or with the inhibitor together with the pro-N6pA probe to avoid any influence of protein expression changes on protein enrichment triggered by the inhibitor (Figure 3A). Additionally, two more controls were included. Cells were treated with plain DMSO or the pro-N6pA probe to check the efficiency of the enrichment in neuroblastoma cells (Figure 3B and Table S4). For each condition, four replicates have been prepared and each enrichment was performed with 400 μg of total protein (Figure 3A). This screening resulted in overall 762 significantly enriched proteins. The control experiment without any inhibitor alone gave 236 significantly enriched proteins. In comparison, the previous agarose beads' enrichment workflow yielded only 14 significantly enriched proteins, marking a large improvement in the enrichment efficiency using the SP2E workflow.[1,17] Together, there is an overlap of 35 proteins, which were significantly enriched under all conditions. The principal component analysis (PCA) showed a clear difference between the DMSO control and probe-treated samples (Figures 3C and S5) for all experiments. Interestingly, the samples that were treated with bafilomycin and monensin clustered together, suggesting a common signaling pathway involving protein AMPylation. This demonstrates the robustness of the SP2E workflow with Pearson correlation coefficients of the LFQ intensities between the replicates over 95% (Figure 3D) and its feasibility to discover new pathways regulating protein AMPylation. The analysis of the enriched proteins revealed the amyloid-β precursor protein (APP) to be one of the top hits in cells treated with bafilomycin and monensin. Further examination of the profile plots showed that APP is only enriched in the cells that were treated with the pro-N6pA probe and either bafilomycin or monensin (Figure 3E). The subsequent search for similar enrichment profiles has uncovered a group of another 12 proteins including GPR56, FAT1, LAMA4, TGOLN2, RNF149, CRIM1, ITM2B, L1CAM, TMEM59, MCAM, LRP1, and CLU that were specifically enriched under these

https://doi.org/10.1021/jacsau.2c00284
JACS Au 2022, 2, 1712−1723

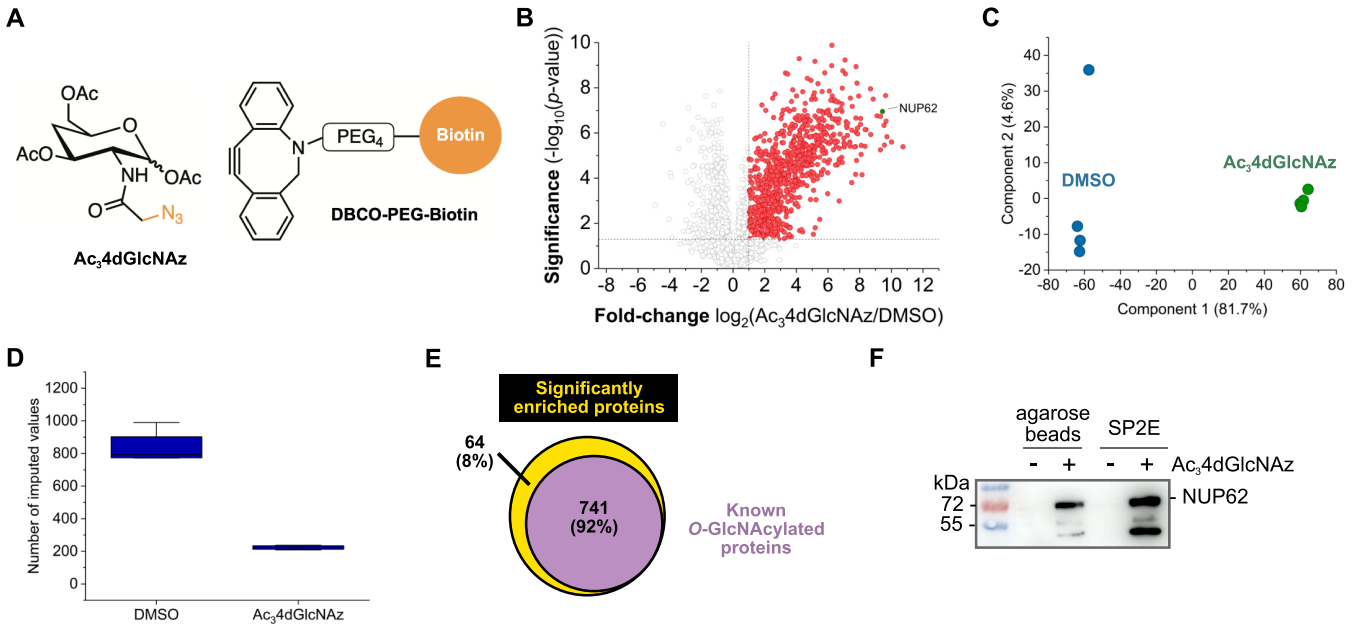

Figure 5. Analysis of *O*-GlcNAcylation by the $Ac_3$4dGlcNAz probe, SPAAC, and SP2E workflow. (A) Chemical structure of the $Ac_3$4dGlcNAz probe for metabolic labeling of *O*-GlcNAcylated proteins and the DBCO−biotin reagent to functionalize the probe-modified proteins by SPAAC. (B) Volcano plot visualizing the enrichment of the *O*-GlcNAcylated proteins; $n = 4$, cutoff lines at p-value >0.05 and 2-fold enrichment. Red dots are significantly enriched proteins. (C) PCA graph points to a clear separation of the control and probe-treated samples. Of note, component 1 possesses a high value of 81.7%. (D) Box plot shows the total number of imputed values across the replicates in DMSO and $Ac_3$4dGlcNAz-treated cells. The number of imputed values indicates how many proteins were not identified in the sample but were found in at least one other sample/replicate. The increased number of imputed values in the DMSO controls demonstrates the efficiency of washing steps removing the nonspecific biding proteins. (E) Diagram showing the overlap between all significantly enriched proteins using the $Ac_3$4dGlcNAz probe and previously described *O*-GlcNAcylated proteins. (F) Enrichment of the modified NUP62 with the agarose-based and the SP2E protocol. In addition, the SP2E enrichment was performed with 400 μg of the protein input. Enriched proteins were released from the streptavidin beads by loading buffer, separated by SDS-PAGE, and analyzed via western blotting with the anti-NUP62 antibody.

two conditions (Figure S5). Interestingly, the lysosomal exonuclease PLD3 has shown a strong response to monensin (Figure 3F). This would point toward the link between AMPylation and trafficking pathways from ER to lysosomes and autophagy.

To investigate the relationship between the monensin concentration and the protein AMPylation stoichiometry in more detail, SH-SY5Y cells were treated with an increasing concentration of monensin in the cell culture media ranging from 2 nM to 2 μM (Figure 4A).[46−48] The concentration of the pro-N6pA probe was kept constant and each condition was performed in duplicate. Surprisingly, the modification of PLD3 increased by 4.0-folds with 2 nM monensin and further increased with a higher inhibitor concentration (Figure 4B and Table S5). The extent of the PLD3 modification was then confirmed in the following in-gel analysis (Figure 4C). Therefore, the SP2E-based enrichment was used, but instead of the protein digest on the beads, they were released from the streptavidin beads, separated on SDS-PAGE, and analyzed by western blotting. For the first time, we uncovered that only the soluble form of PLD3 is modified by the pro-N6pA probe and that there is a strong increase in the modified form upon the addition of monensin and bafilomycin (Figure 4D). The high efficiency of the SP2E workflow is demonstrated by a clear band of soluble PLD3 after enrichment, although this band is not even visible in the western blotting of the whole cell lysate (Figure 4E). In contrast, the modified APP was only found in cells treated with 1 and 2 μM monensin (Figure 4F).[48] Indeed, PTMs of the amyloid-β precursor protein are deemed to play an important role in the development of Alzheimer's disease pathophysiology.[49] By application of our SP2E workflow, we showed that AMPylation might be an additional PTM involved in the regulation of the APP physiological function. Together, the screening of the AMPylation changes triggered by five different active compounds manifests the utility of the SP2E workflow, which is characterized by minimal background binding and robustness.

Application of the SP2E Workflow for Analysis of Protein *O*-GlcNAcylation

To assess the utility of our optimized workflow for other PTMs, we used the previously described $Ac_3$4dGlcNAz probe for the pull-down of *O*-linked β-*N*-acetyl-glucosamine glycosylated (*O*-GlcNAcylation) proteins (Figure 5A).[12,50−52] Numerous metabolic labels have been developed for the characterization of *O*-GlcNAcylated proteins.[51] However, they often suffer from low substrate specificity and labeling efficiency. Here, we used the 2,4-dideoxy-D-glucopyranose derivative, which shows improved specificity for cytosolic proteins.[51] In contrast to previous experiments with the pro-N6pA probe, the $Ac_3$4dGlcNAz probe contains an azide functional group for bioorthogonal protein labeling using SPAAC (Figure 5A).[26] The HeLa cells were treated with a 200 μM final concentration for overnight and lysed. To avoid unspecific reactivity of free thiols with the DBCO−biotin reagent utilized for the SPAAC, they were capped with iodoacetamide.[53] Afterward, the lysate (400 μg total protein) containing *O*-4dGlcNAz proteins was reacted with the DBCO−biotin reagent and enriched using the SP2E method in the same fashion as described above for AMPylation (Figure

https://doi.org/10.1021/jacsau.2c00284
JACS Au 2022, 2, 1712−1723

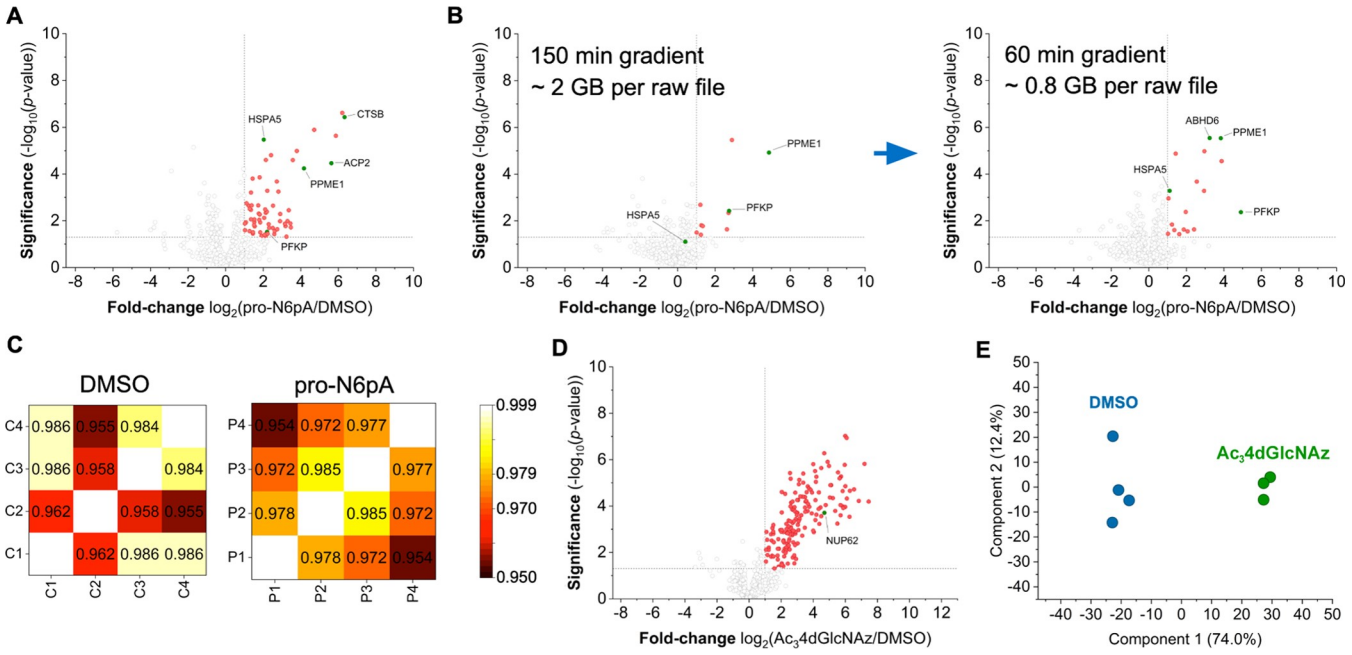

Figure 6. Scale-down of the SP2E workflow into a 96-well plate format. (A) SP2E protocol with 100 μg of the input protein performed in 1.5 mL tubes visualized in the volcano plot. (B) Optimization of the LC-MS/MS measurement with 100 μg protein input using the 96-well plate format SP2E protocol. (C) Heatmaps representing the Pearson correlation coefficients between the replicates. (D) Volcano plot showing the enrichment of *O*-GlcNAcylated proteins starting from 100 μg of the input protein in a 96-well plate format. (E) PCA of the small-scale $Ac_3$4dGlcNAz enrichment shows very good separation of controls from probe-treated samples, with component 1 value corresponding to 74%. All volcano plots, n = 4, cutoff lines at p-value >0.05 and 2-fold enrichment. Red dots are significantly enriched proteins.

5B and Table S6). Interestingly, the high number of significantly enriched proteins leads to a clear separation of the probe-treated and control samples in the PCA plot, with one component over 81% (Figure 5C). Furthermore, the SP2E enrichment of the *O*-GlcNAcylated proteins had a strong impact on the number of imputed values in DMSO-treated control cells (~800) compared to around ~200 values in $Ac_3$4dGlcNAz probe-treated cells. Thus, a high number of proteins was consistently identified only in the probe-treated samples pointing toward a low unspecific protein binding to the magnetic beads (Figure 5D). To our contentment, 92% of the 805 significantly enriched proteins were previously described as *O*-GlcNAcylated (www.oglcnac.mcw.edu), with one of the most significant hits being the well-studied cotranslationally *O*-GlcNAcylated protein NUP62 (Figure 5B–E).[54] To benchmark the enrichment efficiency of the SP2E workflow, we have compared it to the previously used standard workflow, which is based on acetone precipitation and avidin agarose beads. For this purpose, we performed the avidin agarose-based workflow with the same $Ac_3$4dGlcNAz probe-treated lysates and observed that a substantially lower number of proteins was significantly enriched (123, Figure S6). However, 107 (87%) of the protein hits were significantly enriched by both methods, showing a very good fidelity. In addition to the MS-based experiment, we performed a gel-based experiment to benchmark our workflow. Therefore, both methods were performed with 400 μg of starting protein, but instead of digesting the *O*-GlcNAcylated proteins, they were eluted and separated on SDS-PAGE. The enrichment of NUP62 was visualized by an anti-NUP62 antibody on a western blot to demonstrate the comparability of both methods (Figures 5F and S7). Together, these experiments demonstrate the utility of the SP2E protocol for the enrichment of metabolically labeled proteins and the use of different bioorthogonal reactions such as SPAAC.

Scale-Down of the SP2E Workflow into a 96-Well Plate Format

Although the combination of the carboxylate and streptavidin magnetic beads using SP2E streamlined the PTM protein enrichment, it remained to be demonstrated whether this approach is efficient with a lower protein input. Therefore, we performed the enrichment starting with 100 μg of total protein using lysates from pro-N6pA-treated HeLa cells in a standard 1.5 mL eppendorf tube. In this first attempt, it was already possible to significantly enrich five out of six AMPylation marker proteins (Figure 6A and Table S7). Encouraged by the general feasibility of the SP2E workflow with a lower protein input, we have moved on to scale-down the protocol into a 96-well plate format. The dynamic range of the SP2E enrichment efficiency could be shown in the enrichment of rather low abundant AMPylated proteins from pro-N6pA-treated HeLa cells in a 96-well plate format (Figure 6B). The initial testing with a simple decrease of the click reaction volume to 20 μL and wash steps to 150 μL showed only poor enrichment results (Figure S8). Thus, we have adjusted the protocol with the following steps. The clean up of the proteins after the click reaction was extended with an additional acetonitrile washing step, as used for the automated whole proteome sample preparation by Müller et al.[30] In addition, the reduction and alkylation steps were omitted,[55] proteins were digested in 50 μL of triethylammonium bicarbonate (TEAB), and peptides were eluted from the streptavidin magnetic beads with 20 μL of TEAB and 20 μL of 0.5% formic acid (FA) buffer with incubation at 40 °C for 5 min (Figure S8). The resulting MS samples have been acidified by the addition of FA and the peptide mixture was resolved using a 60 min LC-MS/MS

https://doi.org/10.1021/jacsau.2c00284
JACS Au 2022, 2, 1712–1723

measurement (Figure 6B and Table S8). In particular, the use of the shorter gradient is beneficial for two practical reasons. First, more samples can be measured in a shorter time, and second, the MS spectra files are smaller with overall less MS data to the process, leading to faster identification and quantification by search engines. Furthermore, since the total amount of enriched peptides is estimated to be very low, the shorter gradient is likely to result in more intense MS spectra and thus in more identified peptides (Figure 6B). Importantly, the Pearson correlation coefficients of the protein intensities remained over 95% (Figure 6C).

The efficiency of the optimized protocol in a 96-well plate was further tested with the $Ac_3$4dGlcNAz probe (Figure 6D). Indeed, it was possible to significantly enrich 168 proteins including NUP62 among the most significantly enriched ones (Figure 6D and Table S9). In total, 511 proteins were identified. Moreover, both TEAB and ABC buffers used for the digest provided comparable results. To elute the peptides efficiently from the streptavidin magnetic beads after digestion, it is necessary to repeat the elution twice, although it results in peptide dilution in the final MS sample (Figure S8). Similar to the large-scale experiment, the SP2E procedure in the 96-well plate format displays an excellent separation in the PCA of the control and probe-treated samples after enrichment (Figure 6E). To compare the enrichment of NUP62 with the large-scale SP2E workflow, we performed the western blotting analysis of the enriched proteins showing the successful detection of NUP62 using the antibody (Figure S7). In summary, our protocol promises to provide a fast, robust, and high-throughput chemical proteomic platform, which may be used by biologists to assess the PTM status of a wide variety of cells. This is an important prerequisite to unraveling the complex PTM networks and elucidating the underlying functional consequences of protein PTMs.

DISCUSSION

Chemical proteomics has enabled the characterization of many protein PTMs, which are otherwise inaccessible using the whole proteome analysis. Several enrichment workflows have been developed to make the procedure universal and feasible. However, the protocols often require to be carried out by specialized laboratory personnel, they are tedious, and time-consuming. Additionally, with the increasing demand to screen protein PTMs in specialized cell types that are difficult to culture or not accessible in larger amounts typically required by the chemical proteomic protocols, it is of paramount importance to streamline the enrichment workflow and to provide a platform that could be automated. This would parallel the development of the high-throughput automatized whole proteome MS analysis. The transformation of the MS field has been underlined by the rapid improvement in the speed and sensitivity of modern mass spectrometers. The progress of the MS instrumentation has been complemented by software tools allowing for fast and reliable protein identification and quantification. Together, these developments have created a suitable environment for the transition of the chemical proteomic analysis of protein PTMs from a specialized field to a more widely applied analytical tool.

Here, we describe the development and application of the SP2E workflow, which enables the chemical proteomic characterization of protein PTMs in a small-scale, robust, and time-effective manner. The SP2E workflow combines the previously reported protein clean up (SP3) and enrichment protocols.[13,30,33−36] However, each step of the workflow was optimized to enable a smooth transition between the steps and to achieve high identification rates of the enriched proteins. The main difference in the previous MS-based chemical proteomic protocols is the utilization of the paramagnetic beads for both protein clean up and enrichment. It leads to a better separation of the solid and liquid phase and thus improves the removal of nonspecifically binding proteins during the enrichment steps. Furthermore, it allows a better separation in smaller volumes and it can be readily automated. The initial substitution of the standardly used avidin-coated agarose beads with streptavidin-coated magnetic beads resulted in only moderate enrichment of the AMPylated marker proteins. Therefore, we have systematically evaluated each step of the enrichment protocol with a focus on a possible scale-down of the whole procedure. We started our investigation by improving the lysis buffer composition, which is critical to ensure efficient cell lysis already in small volumes to provide protein concentrations of up to 10 μg/μL and to facilitate efficient click chemistry (Figure 2A). Next, enrichment efficiency was improved by spatial separation of protein clean up and enrichment, which allows for more efficient washing and hence less unspecific protein binding. The optimized protocol has been tested in large-scale experiments starting with 400 μg of total protein to explore metabolic and signaling pathways in which protein AMPylation plays a role. In total, 48 samples have been prepared using five different inhibitors and four replicates per condition. We used the same pro-N6pA probe for the optimization of the workflow but SH-SY5Y neuroblastoma cells instead of HeLa cells. The Pearson correlation coefficient of protein intensities among all samples showed a high correlation (>0.95), demonstrating the robustness of the workflow. Interestingly, the PCA revealed a difference between the control and probe-treated cells and importantly displays a clear change in enriched proteins from monensin- and bafilomycin-treated cells, suggesting the specific role of AMPylation in cell stress response to these inhibitors. Moreover, this indicates the high efficiency of the wash steps during the enrichment and reproducibility of the SP2E workflow. Concentration-dependent analysis of monensin on pro-N6pA labeling showed that two replicates of each condition provide sufficient information due to the high reproducibility of the procedure and revealed that the PLD3 modification rapidly increases with a 2 nM monensin concentration.

To show the versatility of the procedure, we have performed the enrichment of *O*-GlcNAcylated proteins using the azido $Ac_3$4dGlcNAz probe. The SPAAC click reaction followed by the SP2E workflow provided excellent enrichment of the well-described glycosylated protein NUP62 with a nominal value of 694-fold enrichment. Furthermore, another 740 known glycosylated proteins were significantly enriched. The outstanding enrichment efficiency is visible by the number of missing values in the control samples (Figure 5D). Since protein glycosylation plays an important role in numerous metabolic processes and often serves as a disease marker, our SP2E protocol offers the possibility to screen for the *O*-GlcNAcylation in a high-throughput manner. This might not only accelerate the progress in the field but also help to decipher the complex glycan patterns by application of different glycosylation labels.

Finally, the current availability of chemical proteomic data shared in public repositories together with the feasibility of

https://doi.org/10.1021/jacsau.2c00284
JACS Au 2022, 2, 1712−1723

sophisticated data analyses necessitates the generation of high-quality data in a high-throughput manner. This can only be achieved by automation of the procedures, for example, with the autoSP3 protocol and other proteomic approaches. Here, we have scaled down the SP2E workflow into the 96-well plate format, which retains the principal operations paralleled in autoSP3. Importantly, we showed by the analysis of protein AMPylation and *O*-GlcNAcylation that 100 μg of the input protein is sufficient for successful PTM protein profiling. This results in the same high correlations between the samples (in average >0.96) and achieves high fold enrichments (NUP62 26-fold and HSPA5 2-fold). Although there is a drop in the overall number of enriched proteins, this is outweighed by cost and time efficiency due to the smaller scale of cell culture, washing steps, usage of the multichannel pipettes, shorter measurement times, and data processing. Of note, in the case of AMPylation, 66% of marker proteins were successfully enriched and for *O*-GlcNAcylation, 167 proteins out of 168 significantly enriched proteins were previously described to be *O*-GlcNAcylated. The main advantage of the SP2E workflow and its application in the 96-well plate format is the possibility to scale down the starting biological material and screen beyond a few dozen samples, which was technically not possible using the previous protocol based on the agarose beads. Overall, the manual SP2E workflow with 24 samples in a 96-well format can be carried out in 3.5−4 h starting from the preparation of the click reaction to the addition of trypsin. After overnight trypsin digest, the peptides are eluted and transferred into MS vials within an additional 45 min.

The limitation of the SP2E workflow for chemical proteomic characterization of protein PTMs is the inherent necessity to treat the cells with small-molecule probes, which are not always commercially available and thus need to be synthesized. Furthermore, the labeling ratio is often determined by the metabolic activation of probes and the substrate selectivity of PTM writers. Thus, it might be difficult to estimate the exact stoichiometry of the protein modification. Similar to other proteomic approaches, the statistical evaluation includes the imputation of missing values, and therefore it might be challenging to identify the hit proteins with low protein intensities as significantly enriched. However, some of these bottlenecks can be overcome by increasing the number of replicates.

The small-scale SP2E allows us to screen many biologically relevant conditions simultaneously. By means of this, metabolic switches which are regulated by PTMs can be identified and subjected to deeper and focused analysis in larger scale. The SP2E workflow is therefore an important step toward robotic automation of chemical proteomics and its broad application to explore complex protein PTM networks to solve biological problems.

METHODS

Culturing of HeLa and SH-SY5Y Cells

HeLa (RRID: CVCL_0030) and SH-SY5Y (RRID: CVCL_0019) cells were cultured in Dulbecco's modified Eagle's medium (DMEM)—high glucose supplemented with 10% fetal calf serum (FCS) and 2 mM l-alanyl-l-glutamine at 37 °C and a 5% CO_2 atmosphere.

Probe Treatments

In each 10 cm dish, 2.5 million HeLa or SH-SY5Y cells were seeded in 10 mL of media. Cells were either treated with 10 μL of a probe (100 mM stock pro-N6pA or 200 mM stock $Ac_3$4dGlcNAz) or with 10 μL of DMSO as a control. After the addition of the probe and the inhibitor, the cells were incubated for 16 h at 37 °C before harvesting. For harvesting, the cells were washed twice with 2 mL of Dulbecco's PBS (DPBS), scraped into 1 mL of DPBS, and pelleted at 1000 rpm, 4 °C.

Cell Lysis

Cells were lysed with 500 μL of lysis buffer (20 mM HEPES, pH 7.5, 1% (v/v) NP-40, 0.2% (w/v) SDS) and sonicated for 10 s at a 20% intensity with a rod sonicator. The lysate was clarified at 11,000 rpm at 4 °C for 10 min and the protein concentration was determined by bicinchoninic acid (BCA) assay.

Measurement of Protein Concentrations

To measure the protein concentrations of the lysates, a bicinchoninic acid assay (Pierce BCA Protein Assay Kit, Thermo Fisher Scientific) was performed. First, bovine serum albumin (BSA) standards with concentrations of 12.5, 25, 50, 100, 200, and 400 μg/mL were prepared and samples as well as controls were diluted 40 times to a total volume of 200 μL. To measure standards, samples, and controls in triplicates, 50 μL of each was added to three wells of a transparent 96-well plate with a flat bottom. Afterward, 100 μL of a working reagent (2 μL of R2 and 98 μL of R1) was added to each well by a multistepper and the plate was incubated for 15 min at 60 °C. Then, the absorbance at 562 nm was measured by Tecan and the protein concentrations were calculated.

Large-Scale SP2E Workflow

A total of 400 μg of protein of probe-treated and control lysates was diluted with lysis buffer (20 mM HEPES, pH 7.5, 1% (v/v) NP-40, 0.2% (w/v) SDS) to a 200 μL reaction volume. To each replicate, 2 μL of biotin−PEG−N_3 (10 mM in DMSO), 2 μL of TCEP (100 mM in water), and 0.25 μL of tris((1-benzyl-4-triazolyl)methyl)amine (TBTA) (83.5 mM in DMSO) were added. Samples were gently vortexed, and the click reaction was initiated by the addition of 4 μL of $CuSO_4$ (50 mM in water) and incubated for 1.5 h (room temperature (rt), 600 rpm). Subsequently, 200 μL of 8 M urea was added to each replicate. A total of 100 μL of mixed hydrophobic and hydrophilic carboxylate-coated magnetic beads (1:1) was washed thrice with 500 μL of water. The click reaction mixture was directly transferred onto the equilibrated carboxylate-coated magnetic beads, resuspended, and 600 μL of ethanol was added. After resuspending the beads via vortexing, the suspension was incubated for 5 min at rt and 950 rpm. The beads were washed thrice with 500 μL of 80% ethanol in water using a magnetic rack and the proteins were separately eluted by the addition of 0.5 mL of 0.2% SDS in PBS. For this, the beads were resuspended, incubated for 5 min at 950 rpm, rt, and the supernatant was directly transferred onto 50 μL of equilibrated streptavidin-coated magnetic beads (three times prewashed with 500 μL of 0.2% SDS in PBS). The procedure was repeated once and the supernatants were combined and incubated for 1 h, rt and 950 rpm for biotin/streptavidin binding. The streptavidin-coated magnetic bead mixture was washed thrice with 500 μL of 0.1% NP-40 in PBS, twice with 500 μL of 6 M urea, and twice with 500 μL of water. Washed bead mixtures were resuspended in 80 μL of 125 mM ABC buffer, and proteins were reduced and alkylated by the addition of 10 μL of 100 mM TCEP and 10 μL of 400 mM chloracetamide, followed by 5 min incubation at 95 °C. Proteins were digested overnight at 37 °C with 1.5 μL of sequencing grade trypsin (0.5 mg/mL). The following day, the beads were washed thrice with 100 μL of 100 mM ABC buffer and the supernatants were combined and acidified with 2 μL of formic acid. Peptides were desalted using 50 mg of Sep-Pak C18 cartridges on a vacuum manifold. The columns were equilibrated with 1 mL of acetonitrile, 1 mL of elution buffer (80% acetonitrile with 0.5% formic acid in water), and 3 mL of wash buffer (0.5% formic acid in water). Subsequently, the samples were loaded on the cartridges and washed with 3 mL of wash buffer. The peptides were eluted two times with 250 μL of elution buffer and vacuum-dried with a SpeedVac at 35 °C. Finally, dried peptides were

https://doi.org/10.1021/jacsau.2c00284
JACS Au 2022, 2, 1712−1723

reconstituted in 30 μL of 1% formic acid in water by vortexing and sonication (15 min) and transferred to an MS vial.

Small-Scale SP2E Workflow

A total of 100 μg of protein of probe-treated and control lysates was diluted with lysis buffer (20 mM HEPES, pH 7.5, 1% (v/v) NP-40, 0.2% (w/v) SDS) to a 19 μL reaction volume in a 96-well plate. The master mix containing 0.2 μL of biotin−PEG−N_3 (10 mM in DMSO), 0.2 μL of TCEP (100 mM in water), and 0.125 μL of TBTA (16.7 mM in DMSO) was added to each sample. Samples were gently vortexed and the click reaction was initiated by the addition of 0.4 μL of $CuSO_4$ (50 mM in water) and incubated for 1.5 h (rt, 600 rpm). Subsequently, 60 μL of 8 M urea was added to each replicate. A total of 100 μL of mixed hydrophobic and hydrophilic carboxylate-coated magnetic beads (1:1) were washed thrice with 100 μL of water. The click reaction mixture was directly transferred onto the equilibrated carboxylate-coated magnetic beads, resuspended, and 100 μL of absolute ethanol was added. After resuspending the beads via vortexing, the suspension was incubated for 5 min at rt and 950 rpm. The beads were washed thrice with 150 μL of 80% ethanol in water using a magnetic rack and once with 150 μL of acetonitrile (LC-MS). Proteins were separately eluted by the addition of 60 μL of 0.2% SDS in PBS. For this, the beads were resuspended, incubated for 5 min at 40 °C and 950 rpm, and the supernatant was directly transferred onto 50 μL of equilibrated streptavidin-coated magnetic beads (three times prewashed with 100 μL of 0.2% SDS in PBS). The procedure was repeated twice, and the supernatants were combined and incubated for 1 h at rt and 800 rpm for biotin/streptavidin binding. The streptavidin-coated magnetic bead mixture was washed thrice with 150 μL of 0.1% NP-40 in PBS, twice with 150 μL of 6 M urea, and twice with 150 μL of water. For each washing step, the beads were incubated 1 min at rt and 800 rpm. Washed bead mixtures were resuspended in 50 μL of 50 mM TEAB and proteins were digested overnight at 37 °C by addition of 1.5 μL of sequencing grade trypsin (0.5 mg/mL). The following day, the beads were washed twice with 20 μL of 50 mM TEAB buffer and twice with 20 μL of 0.5% FA and the wash fractions were collected and combined. For each washing step, the beads were incubated for 5 min at 40 °C and 600 rpm. The combined washed fractions were acidified by the addition of 0.9 μL of formic acid (FA) and transferred directly without desalting to an MS vial.

Large-Scale SPAAC Protocol

A total of 400 μg of protein of probe-treated and control lysates was diluted with lysis buffer (20 mM HEPES, pH 7.5, 1% (v/v) NP-40, 0.2% (w/v) SDS) to a 200 μL reaction volume. To each replicate, 3 μL of 1 M IAA in water was added and incubated for 30 min at 750 rpm, 25 °C. Next, 2 μL of a 2 mM DBCO−PEG−N_3 reagent was added to initiate the SPAAC reaction. The reaction mixtures were incubated at 25 °C, 750 rpm for 30 min. The samples proceeded further in the same way as for CuAAC.

Small-Scale SPAAC Protocol

A total of 100 μg of protein of probe-treated and control lysates was diluted with lysis buffer (20 mM HEPES, pH 7.5, 1% (v/v) NP-40, 0.2% (w/v) SDS) to a 19 μL reaction volume in a 96-well plate. To each replicate, 0.3 μL of 1 M IAA in water was added and incubated for 30 min at 750 rpm, 25 °C. Next, 0.2 μL of the 2 mM DBCO−PEG−N_3 reagent was added to initiate the SPAAC reaction. The reaction mixtures were incubated at 25 °C, 750 rpm for 30 min. The samples proceeded further in the same way as for CuAAC.

ASSOCIATED CONTENT

Supporting Information

The Supporting Information is available free of charge at https://pubs.acs.org/doi/10.1021/jacsau.2c00284.

Supporting figures, cell culture conditions, SP2E workflow, LC-MS/MS acquisition conditions, data analysis, and list of reagents (PDF)

AUTHOR INFORMATION

Corresponding Author

Pavel Kielkowski − *Institute for Chemical Epigenetics Munich, LMU Munich, 81375 Munich, Germany;* orcid.org/0000-0003-4910-6263; Email: pavel.kielkowski@cup.lmu.de

Authors

Tobias Becker − *Institute for Chemical Epigenetics Munich, LMU Munich, 81375 Munich, Germany*

Andreas Wiest − *Institute for Chemical Epigenetics Munich, LMU Munich, 81375 Munich, Germany;* orcid.org/0000-0003-2525-6304

András Telek − *Institute for Chemical Epigenetics Munich, LMU Munich, 81375 Munich, Germany*

Daniel Bejko − *Institute for Chemical Epigenetics Munich, LMU Munich, 81375 Munich, Germany*

Anja Hoffmann-Röder − *Department of Chemistry, LMU Munich, 81377 Munich, Germany;* orcid.org/0000-0002-8352-8323

Complete contact information is available at: https://pubs.acs.org/10.1021/jacsau.2c00284

Author Contributions

P.K. designed the method; A.W., A.T., and D.B. performed the experiments and contributed to the optimization of the method; T.B. carried out the AMPylation study; A H.-R. provided the $Ac_3$4dGlcNAz probe and contributed to *O*-GlcNAcylation; T.B. and P.K. overviewed the study and analyzed the data; and T.B. and P.K. wrote the manuscript with input from all authors.

Notes

The authors declare no competing financial interest.

Proteomics data are freely available at ProteomeXchange Consortium via PRIDE partner repository with the data set identifier PXD033644. Tables S1−S14 are available via figshare data repository DOI: 10.6084/m9.figshare.19969907.

ACKNOWLEDGMENTS

This research project was supported by Liebig fellowship from VCI to P.K. and T.B., LMUexcellence Junior Fund to P.K., and generous support from SFB1309 by DFG. The authors thank Stefan Marchner (LMU Munich) for the preparation of the $Ac_3$4dGlcNAz probe and Dietrich Mostert (Technical University of Munich) for proofreading.

REFERENCES

(1) Becker, T.; Cappel, C.; Matteo, F. D.; Sonsalla, G.; Kaminska, E.; Spada, F.; Cappello, S.; Damme, M.; Kielkowski, P. AMPylation Profiling during Neuronal Differentiation Reveals Extensive Variation on Lysosomal Proteins. *iScience* **2021**, *24*, No. 103521.

(2) Mansfield, S. G.; Gordon-Weeks, P. R. Dynamic Post-Translational Modification of Tubulin in Rat Cerebral Cortical Neurons Extending Neurites in Culture: Effects of Taxol. *J. Neurocytol.* **1991**, *20*, 654−666.

(3) Zheng, P.; Obara, C. J.; Szczesna, E.; Nixon-Abell, J.; Mahalingan, K. K.; Roll-Mecak, A.; Lippincott-Schwartz, J.; Blackstone, C. ER Proteins Decipher the Tubulin Code to Regulate Organelle Distribution. *Nature* **2022**, 132−138.

(4) Aebersold, R.; Agar, J. N.; Amster, I. J.; Baker, M. S.; Bertozzi, C. R.; Boja, E. S.; Costello, C. E.; Cravatt, B. F.; Fenselau, C.; Garcia, B. A.; Ge, Y.; Gunawardena, J.; Hendrickson, R. C.; Hergenrother, P. J.;

Huber, C. G.; Ivanov, A. R.; Jensen, O. N.; Jewett, M. C.; Kelleher, N. L.; Kiessling, L. L.; Krogan, N. J.; Larsen, M. R.; Loo, J. A.; Loo, R. R. O.; Lundberg, E.; MacCoss, M. J.; Mallick, P.; Mootha, V. K.; Mrksich, M.; Muir, T. W.; Patrie, S. M.; Pesavento, J. J.; Pitteri, S. J.; Rodriguez, H.; Saghatelian, A.; Sandoval, W.; Schlüter, H.; Sechi, S.; Slavoff, S. A.; Smith, L. M.; Snyder, M. P.; Thomas, P. M.; Uhlén, M.; Eyk, J. E. V.; Vidal, M.; Walt, D. R.; White, F. M.; Williams, E. R.; Wohlschlager, T.; Wysocki, V. H.; Yates, N. A.; Young, N. L.; Zhang, B. How Many Human Proteoforms Are There? *Nat. Chem. Biol.* **2018**, *14*, 206−214.

(5) Brüning, F.; Noya, S. B.; Bange, T.; Koutsouli, S.; Rudolph, J. D.; Tyagarajan, S. K.; Cox, J.; Mann, M.; Brown, S. A.; Robles, M. S. Sleep-Wake Cycles Drive Daily Dynamics of Synaptic Phosphorylation. *Science* **2019**, *366*, No. eaav3617.

(6) Truttmann, M. C.; Pincus, D.; Ploegh, H. L. Chaperone AMPylation Modulates Aggregation and Toxicity of Neurodegenerative Disease-Associated Polypeptides. *Proc. Natl. Acad. Sci. U.S.A.* **2018**, *115*, No. 201801989.

(7) Rogowski, K.; van Dijk, J.; Magiera, M. M.; Bosc, C.; Deloulme, J.-C.; Bosson, A.; Peris, L.; Gold, N. D.; Lacroix, B.; Grau, M. B.; Bec, N.; Larroque, C.; Desagher, S.; Holzer, M.; Andrieux, A.; Moutin, M.-J.; Janke, C. A Family of Protein-Deglutamylating Enzymes Associated with Neurodegeneration. *Cell* **2010**, *143*, 564−578.

(8) Hoch, N. C.; Polo, L. M. ADP-Ribosylation: From Molecular Mechanisms to Human Disease. *Genet. Mol. Biol.* **2020**, *43*, No. e20190075.

(9) Kam, T.-I.; Mao, X.; Park, H.; Chou, S.-C.; Karuppagounder, S. S.; Umanah, G.; Yun, S.; Brahmachari, S.; Panicker, N.; Chen, R.; Andrabi, S. A.; Qi, C.; Poirier, G. G.; Pletnikova, O.; Troncoso, J. C.; Bekris, L. M.; Leverenz, J. B.; Pantelyat, A.; Ko, H.; Rosenthal, L. S.; Dawson, T. M.; Dawson, V. L. Poly(ADP-Ribose) Drives Pathologic α-Synuclein Neurodegeneration in Parkinson's Disease. *Science* **2018**, *362*, No. eaat8407.

(10) Smith, L. M.; Thomas, P. M.; Shortreed, M. R.; Schaffer, L. V.; Fellers, R. T.; LeDuc, R. D.; Tucholski, T.; Ge, Y.; Agar, J. N.; Anderson, L. C.; Chamot-Rooke, J.; Gault, J.; Loo, J. A.; Paša-Tolić, L.; Robinson, C. V.; Schlüter, H.; Tsybin, Y. O.; Vilaseca, M.; Vizcaíno, J. A.; Danis, P. O.; Kelleher, N. L. A Five-Level Classification System for Proteoform Identifications. *Nat. Method* **2019**, *16*, 939−940.

(11) Smith, L. M.; Agar, J. N.; Chamot-Rooke, J.; Danis, P. O.; Ge, Y.; Loo, J. A.; Paša-Tolić, L.; Tsybin, Y. O.; Kelleher, N. L.; The Consortium for Top-Down Proteomics. The Human Proteoform Project: Defining the Human Proteome. *Sci. Adv.* **2021**, *7*, No. eabk0734.

(12) Laughlin, S. T.; Bertozzi, C. R. Metabolic Labeling of Glycans with Azido Sugars and Subsequent Glycan-Profiling and Visualization via Staudinger Ligation. *Nat. Protoc.* **2007**, *2*, 2930−2944.

(13) Kallemeijn, W. W.; Lanyon-Hogg, T.; Panyain, N.; Grocin, A. G.; Ciepla, P.; Morales-Sanfrutos, J.; Tate, E. W. Proteome-Wide Analysis of Protein Lipidation Using Chemical Probes: In-Gel Fluorescence Visualization, Identification and Quantification of N-Myristoylation, N- and S-Acylation, O-Cholesterylation, S-Farnesylation and S-Geranylgeranylation. *Nat. Protoc.* **2021**, *16*, 5083−5122.

(14) Martin, B. R.; Wang, C.; Adibekian, A.; Tully, S. E.; Cravatt, B. F. Global Profiling of Dynamic Protein Palmitoylation. *Nat. Method* **2012**, *9*, 84−89.

(15) Parker, C. G.; Pratt, M. R. Click Chemistry in Proteomic Investigations. *Cell* **2020**, *180*, 605−632.

(16) Kielkowski, P.; Buchsbaum, I. Y.; Becker, T.; Bach, K.; Cappello, S.; Sieber, S. A. A Pronucleotide Probe for Live-Cell Imaging of Protein AMPylation. *ChemBioChem* **2020**, *21*, 1285−1287.

(17) Kielkowski, P.; Buchsbaum, I. Y.; Kirsch, V. C.; Bach, N. C.; Drukker, M.; Cappello, S.; Sieber, S. A. FICD Activity and AMPylation Remodelling Modulate Human Neurogenesis. *Nat. Commun.* **2020**, *11*, No. 517.

(18) Sinha, A.; Mann, M. A Beginner's Guide to Mass Spectrometry−Based Proteomics. *Biochemist* **2020**, *42*, 64−69.

(19) Cox, J.; Mann, M. MaxQuant Enables High Peptide Identification Rates, Individualized p.p.b.-Range Mass Accuracies and Proteome-Wide Protein Quantification. *Nat. Biotechol.* **2008**, *26*, 1367−1372.

(20) Tyanova, S.; Temu, T.; Sinitcyn, P.; Carlson, A.; Hein, M. Y.; Geiger, T.; Mann, M.; Cox, J. The Perseus Computational Platform for Comprehensive Analysis of (Prote)Omics Data. *Nat. Method* **2016**, *13*, 731−740.

(21) Yu, F.; Teo, G. C.; Kong, A. T.; Haynes, S. E.; Avtonomov, D. M.; Geiszler, D. J.; Nesvizhskii, A. I. Identification of Modified Peptides Using Localization-Aware Open Search. *Nat. Commun.* **2020**, *11*, No. 4065.

(22) Grammel, M.; Luong, P.; Orth, K.; Hang, H. C. A Chemical Reporter for Protein AMPylation. *J. Am. Chem. Soc.* **2011**, *133*, 17103−17105.

(23) Kliza, K. W.; Liu, Q.; Roosenboom, L. W. M.; Jansen, P. W. T. C.; Filippov, D. V.; Vermeulen, M. Reading ADP-Ribosylation Signaling Using Chemical Biology and Interaction Proteomics. *Mol. Cell* **2021**, *81*, 4552.e8−4567.e8.

(24) Yang, Y.-Y.; Ascano, J. M.; Hang, H. C. Bioorthogonal Chemical Reporters for Monitoring Protein Acetylation. *J. Am. Chem. Soc.* **2010**, *132*, 3640−3641.

(25) Sieber, S. A.; Cappello, S.; Kielkowski, P. From Young to Old: AMPylation Hits the Brain. *Cell. Chem. Biol.* **2020**, *27*, 773−779.

(26) Agard, N. J.; Prescher, J. A.; Bertozzi, C. R. A Strain-Promoted [3 + 2] Azide−Alkyne Cycloaddition for Covalent Modification of Biomolecules in Living Systems. *J. Am. Chem. Soc.* **2004**, *126*, 15046−15047.

(27) Zecha, J.; Satpathy, S.; Kanashova, T.; Avanessian, S. C.; Kane, M. H.; Clauser, K. R.; Mertins, P.; Carr, S. A.; Kuster, B. TMT Labeling for the Masses: A Robust and Cost-Efficient, In-Solution Labeling Approach* [S]. *Mol. Cell. Proteomics* **2019**, *18*, 1468−1478.

(28) Cox, J.; Hein, M. Y.; Luber, C. A.; Paron, I.; Nagaraj, N.; Mann, M. Accurate Proteome-Wide Label-Free Quantification by Delayed Normalization and Maximal Peptide Ratio Extraction, Termed MaxLFQ. *Mol. Cell. Proteomics* **2014**, *13*, 2513−2526.

(29) Wiśniewski, J. R.; Zougman, A.; Nagaraj, N.; Mann, M. Universal Sample Preparation Method for Proteome Analysis. *Nat. Method* **2009**, *6*, 359−362.

(30) Müller, T.; Kalxdorf, M.; Longuespée, R.; Kazdal, D. N.; Stenzinger, A.; Krijgsveld, J. Automated Sample Preparation with SP3 for Low-input Clinical Proteomics. *Mol. Syst. Biol.* **2020**, *16*, No. e9111.

(31) Hughes, C. S.; Moggridge, S.; Müller, T.; Sorensen, P. H.; Morin, G. B.; Krijgsveld, J. Single-Pot, Solid-Phase-Enhanced Sample Preparation for Proteomics Experiments. *Nat. Protoc.* **2019**, *14*, 68−85.

(32) Sielaff, M.; Kuharev, J.; Bohn, T.; Hahlbrock, J.; Bopp, T.; Tenzer, S.; Distler, U. Evaluation of FASP, SP3, and IST Protocols for Proteomic Sample Preparation in the Low Microgram Range. *J. Proteome Res.* **2017**, *16*, 4060−4072.

(33) Wright, M. H.; Clough, B.; Rackham, M. D.; Rangachari, K.; Brannigan, J. A.; Grainger, M.; Moss, D. K.; Bottrill, A. R.; Heal, W. P.; Broncel, M.; Serwa, R. A.; Brady, D.; Mann, D. J.; Leatherbarrow, R. J.; Tewari, R.; Wilkinson, A. J.; Holder, A. A.; Tate, E. W. Validation of N-Myristoyltransferase as an Antimalarial Drug Target Using an Integrated Chemical Biology Approach. *Nat. Chem.* **2014**, *6*, 112−121.

(34) Yan, T.; Desai, H. S.; Boatner, L. M.; Yen, S. L.; Cao, J.; Palafox, M. F.; Jami-Alahmadi, Y.; Backus, K. SP3-FAIMS Chemoproteomics for High Coverage Profiling of the Human Cysteinome. *ChemBioChem* **2021**, *22*, 1841−1851.

(35) Klont, F.; Kwiatkowski, M.; Faiz, A.; van den Bosch, T.; Pouwels, S. D.; Dekker, F. J.; ten Hacken, N. H. T.; Horvatovich, P.; Bischoff, R. Adsorptive Microtiter Plates As Solid Supports in Affinity Purification Workflows. *J. Proteome Res.* **2021**, *20*, 5218−5221.

(36) Makowski, M. M.; Gräwe, C.; Foster, B. M.; Nguyen, N. V.; Bartke, T.; Vermeulen, M. Global Profiling of Protein−DNA and

https://doi.org/10.1021/jacsau.2c00284
JACS Au 2022, 2, 1712−1723

Protein−Nucleosome Binding Affinities Using Quantitative Mass Spectrometry. *Nat. Commun.* **2018**, *9*, No. 1653.
(37) Tian, Y.-P.; Zhang, X.-J.; Wu, J.-Y.; Fun, H.-K.; Jiang, M.-H.; Xu, Z.-Q.; Usman, A.; Chantrapromma, S.; Thompson, L. K. Structural Diversity and Properties of a Series of Dinuclear and Mononuclear Copper(Ii) and Copper(i) Carboxylato Complexes. *New J. Chem.* **2002**, *26*, 1468−1473.
(38) Stojceva Radovanovic, B. C.; Premovic, P. I. Thermal Behaviour of Cu(II)-Urea Complex. *J. Therm. Anal.* **1992**, *38*, 715−719.
(39) Hughes, C. S.; Foehr, S.; Garfield, D. A.; Furlong, E. E.; Steinmetz, L. M.; Krijgsveld, J. Ultrasensitive Proteome Analysis Using Paramagnetic Bead Technology. *Mol. Syst. Biol.* **2014**, *10*, 757.
(40) Truttmann, M. C.; Zheng, X.; Hanke, L.; Damon, J. R.; Grootveld, M.; Krakowiak, J.; Pincus, D.; Ploegh, H. L. Unrestrained AMPylation Targets Cytosolic Chaperones and Activates the Heat Shock Response. *Proc. Natl. Acad. Sci. U.S.A.* **2017**, *114*, E152−E160.
(41) Sanyal, A.; Dutta, S.; Camara, A.; Chandran, A.; Koller, A.; Watson, B. G.; Sengupta, R.; Ysselstein, D.; Montenegro, P.; Cannon, J.; Rochet, J.-C.; Mattoo, S. Alpha-Synuclein Is a Target of Fic-Mediated Adenylylation/AMPylation: Possible Implications for Parkinson's Disease. *J. Mol. Biol.* **2019**, *431*, 2266−2282.
(42) Raught, B.; Gingras, A.-C.; Sonenberg, N. The Target of Rapamycin (TOR) Proteins. *Proc. Natl. Acad. Sci. U.S.A.* **2001**, *98*, 7037−7044.
(43) Leeman, D. S.; Hebestreit, K.; Ruetz, T.; Webb, A. E.; McKay, A.; Pollina, E. A.; Dulken, B. W.; Zhao, X.; Yeo, R. W.; Ho, T. T.; Mahmoudi, S.; Devarajan, K.; Passegué, E.; Rando, T. A.; Frydman, J.; Brunet, A. Lysosome Activation Clears Aggregates and Enhances Quiescent Neural Stem Cell Activation during Aging. *Science* **2018**, *359*, 1277−1283.
(44) Yoshimori, T.; Yamamoto, A.; Moriyama, Y.; Futai, M.; Tashiro, Y. Bafilomycin A1, a Specific Inhibitor of Vacuolar-Type H(+)-ATPase, Inhibits Acidification and Protein Degradation in Lysosomes of Cultured Cells. *J. Biol. Chem.* **1991**, *266*, 17707−17712.
(45) Zhang, J.-G.; Fariss, M. W. Thenoyltrifluoroacetone, a Potent Inhibitor of Carboxylesterase Activity. *Biochem. Pharmacol.* **2002**, *63*, 751−754.
(46) Mollenhauer, H. H.; Morré, D. J.; Rowe, L. D. Alteration of Intracellular Traffic by Monensin; Mechanism, Specificity and Relationship to Toxicity. *Biochim. Biophys. Acta, Rev. Biomembr.* **1990**, *1031*, 225−246.
(47) Pohlmann, R.; Krüger, S.; Hasilik, A.; von Figura, K. Effect of Monensin on Intracellular Transport and Receptor-Mediated Endocytosis of Lysosomal Enzymes. *Biochem. J.* **1984**, *217*, 649−658.
(48) Wang, X.; Wu, X.; Zhang, Z.; Ma, C.; Wu, T.; Tang, S.; Zeng, Z.; Huang, S.; Gong, C.; Yuan, C.; Zhang, L.; Feng, Y.; Huang, B.; Liu, W.; Zhang, B.; Shen, Y.; Luo, W.; Wang, X.; Liu, B.; Lei, Y.; Ye, Z.; Zhao, L.; Cao, D.; Yang, L.; Chen, X.; Haydon, R. C.; Luu, H. H.; Peng, B.; Liu, X.; He, T.-C. Monensin Inhibits Cell Proliferation and Tumor Growth of Chemo-Resistant Pancreatic Cancer Cells by Targeting the EGFR Signaling Pathway. *Sci. Rep.* **2018**, *8*, No. 17914.
(49) Long, J. M.; Holtzman, D. M. Alzheimer Disease: An Update on Pathobiology and Treatment Strategies. *Cell* **2019**, *179*, 312−339.
(50) Yang, X.; Qian, K. Protein *O*-GlcNAcylation: Emerging Mechanisms and Functions. *Nat. Rev. Mol. Cell Biol.* **2017**, *18*, 452−465.
(51) Li, J.; Wang, J.; Wen, L.; Zhu, H.; Li, S.; Huang, K.; Jiang, K.; Li, X.; Ma, C.; Qu, J.; Parameswaran, A.; Song, J.; Zhao, W.; Wang, P. G. An OGA-Resistant Probe Allows Specific Visualization and Accurate Identification of O -GlcNAc-Modified Proteins in Cells. *ACS Chem. Biol.* **2016**, *11*, 3002−3006.
(52) Pedowitz, N. J.; Pratt, M. R. Design and Synthesis of Metabolic Chemical Reporters for the Visualization and Identification of Glycoproteins. *RSC Chem. Biol.* **2021**, *2*, 306−321.
(53) Zhang, C.; Zhang, C.; Dai, P.; Vinogradov, A.; Gates, Z. Site-Selective Cysteine-Cyclooctyne Conjugation. *Angew. Chem., Int. Ed.* **2018**, *57*, 6459−6463.
(54) Wulff-Fuentes, E.; Berendt, R. R.; Massman, L.; Danner, L.; Malard, F.; Vora, J.; Kahsay, R.; Stichelen, S. O.-V. The Human O-GlcNAcome Database and Meta-Analysis. *Sci. Data* **2021**, *8*, No. 25.
(55) Petelski, A. A.; Emmott, E.; Leduc, A.; Huffman, R. G.; Specht, H.; Perlman, D. H.; Slavov, N. Multiplexed Single-Cell Proteomics Using SCoPE2. *Nat. Protoc.* **2021**, *16*, 5398−5425.

https://doi.org/10.1021/jacsau.2c00284
JACS Au 2022, 2, 1712−1723